Applied Catalysis B: Environmental 179 (2015) 69–77

Contents lists available at ScienceDirect

Applied Catalysis B: Environmental

journal homepage: www.elsevier.com/locate/apcatb

# In-situ regeneration of Au nanocatalysts by atmospheric-pressure air plasma: Significant contribution of water vapor

Bin Zhu[a,b], Xiao-Song Li[a,b], Jing-Lin Liu[a,b], Jin-Bao Liu[a,b], Xiaobing Zhu[a,b,*], Ai-Min Zhu[a,b,*]

[a] Laboratory of Plasma Physical Chemistry, Dalian University of Technology, Dalian 116024, China
[b] Center for Hydrogen Energy and Liquid Fuels, Dalian University of Technology, Dalian 116024, China

ARTICLE INFO

*Article history:*
Received 27 January 2015
Received in revised form 6 May 2015
Accepted 7 May 2015
Available online 8 May 2015

*Keywords:*
Au catalyst
Air plasma
In-situ regeneration
Water vapor
CO oxidation

ABSTRACT

In-situ regeneration of deactivated Au nanocatalysts during CO oxidation, was conducted effectively by pure oxygen plasma, but poisoned by dry air plasma in our previous work (*Appl. Catal. B* **2012**, *119–120*, 49–55). With extension of previous study, a simple and effective technique of atmospheric-pressure cold plasma of humid air is explored for in-situ regeneration of Au nanocatalysts. In comparison with ineffective regeneration by dry plasma, humid plasma using synthetic air (20% $O_2$ balance $N_2$) as discharge gas surprisingly exhibited effective regeneration performance over Au catalyst due to significant contribution of water vapor. After plasma regeneration for 5 min, the regeneration degree of Au catalysts significantly increased up to 98% under humid plasma in presence of 2.77 vol.% water, while decreased down to negative 29% under dry plasma. To disclose the mechanism of water vapor contribution to greatly improved regeneration degree, the characterizations of regenerated catalysts, and the analyses of electric discharge characteristics and gaseous products during the plasma regeneration were conducted. The significant contribution of water vapor embodies in that it speeds up the decomposition of carbonate species and simultaneously inhibits the formation of poisoning species of nitrogen oxides. Furthermore, normal air instead of synthetic air in humid plasma regeneration was implemented on the evaluations of the deactivated Au catalysts after a long-term reaction and during ten deactivation-regeneration cycles, which ensured the feasibility and reliability of in-situ plasma regeneration of Au nanocatalysts as a simple, effective and promising technique.



## 1. Introduction

Supported gold (Au) catalysts have been intensively investigated for catalyzing a wide variety of reactions at relatively mild conditions in the past decades [1–5]. Due to its superior activity on CO oxidation at low temperature [6–8], Au catalyst is expected as an excellent candidate for environmental protection [9–12], such as indoor air purification and canister respirators. Unfortunately, the practical applications of Au catalyst still remain a big problem because it shows a gradual deactivation with time on stream (TOS) [13–15]. Currently, agglomeration of Au particles and accumulation of carbonate species on catalyst surface are generally considered as the two major reasons for the deactivation phenomenon [16,17]. Meanwhile, for CO oxidation over Au catalysts at low temperature, the deactivation is mainly caused by the reversible surface carbonate species accumulating rather than the irreversible Au nanoparticle aggregating. The surface carbonate species on the deactivated Au catalysts can be decomposed or removed by heat-treatment [15,16,18]. However, the conventional heat-treatment method is prone to bring a negative effect of Au nanoparticles aggregation.

A promising alternative technique is the cold plasma (abbreviated as plasma below) [19–21], in which the interaction of active species (e.g. electrons, ions and radicals) with Au catalyst could effectively remove the accumulated carbonate species from catalyst surface at low temperature. Although various plasma techniques have been employed to prepare or modify Au catalysts [22,23], few works on plasma regeneration of Au catalysts were reported [17,24]. Our previous work demonstrated that pure oxygen plasma is a fast and effective approach to in-situ regenerate Au/$TiO_2$ nanocatalyst [24]. Undoubtedly, as a discharge gas of plasma regeneration, air is far easier accessible and much cheaper

* Corresponding authors at: Laboratory of Plasma Physical Chemistry, Dalian University of Technology, Dalian 116024, China. Tel.: +86 411 84706094; fax: +86 411 84706094.
*E-mail addresses:* xzhu@dlut.edu.cn (X. Zhu), amzhu@dlut.edu.cn (A.-M. Zhu).

http://dx.doi.org/10.1016/j.apcatb.2015.05.020
0926-3373/

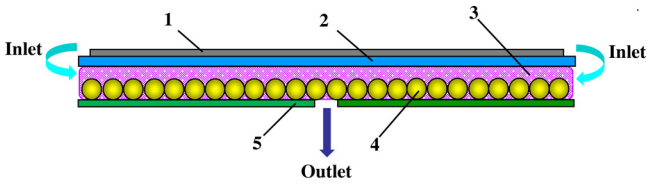


**Fig. 1.** Schematic diagram of the catalyst-packed DBD reactor. 1 – high-voltage electrode, 2 – quartz disc, 3 – plasma zone, 4 – $Au/TiO_2$ catalysts, 5 – grounded electrode.

than pure oxygen. However, the presence of nitrogen in air causes a side effect of extra poisoning towards Au catalyst due to nitrogen oxides produced in air plasma [24], which suppresses the technique of air plasma regeneration of Au catalyst. Inspired by the literatures [25–27], the presence of water vapor in air plasma can effectively inhibit the formation of nitrogen oxides, which might be a simple and feasible solution to avoid the poison effect of nitrogen oxides on Au catalysts during air plasma regeneration. Meanwhile, regeneration efficiency of the air plasma could also be improved by water vapor, due to that water vapor favors the decomposition of surface carbonate species [18,28–34].

In this paper, with extension of previous work [24], we demonstrate a simple and effective technique of atmospheric-pressure cold plasma of humid air instead of pure oxygen or dry air, for in-situ regeneration of deactivated $Au/TiO_2$ nanocatalysts, which features a rapid regeneration of Au catalyst and the elimination of extra poisoning of nitrogen oxides produced in dry air plasma on Au catalyst. Moreover, the significant contribution of water vapor to the regeneration of Au catalysts in air plasma was disclosed, for which the mechanism was further discussed.

## 2. Experimental

### 2.1. Catalyst preparation, reactor and catalytic activity evaluation

A nominal 1 wt.% Au catalyst was prepared by a modified impregnation method [35]. A 4.3 mL aqueous $HAuCl_4$ solution ($2.43 \times 10^{-2}$ mol/L) was slowly added to 2 g $TiO_2$ powder (Degussa P25) under manual stirring. The slurry was aged at room temperature for 18 h, and rinsed twice with an aqueous ammonia solution (pH 8) and another twice with deionized water to remove residual chloride ions. After rinsing, the filtered cake was dried in air at 80 °C for 6 h and calcined at 300 °C for 2 h to obtain the $Au/TiO_2$ catalyst.

CO oxidation reaction over $Au/TiO_2$ catalyst and in-situ regeneration of the $Au/TiO_2$ catalyst were conducted in a home-made dielectric barrier discharge (DBD) reactor of planar configuration, as shown in Fig. 1. The DBD reactor consists of a high-voltage electrode of 20 mm in diameter, a grounded electrode and a quartz disc of 40 mm in diameter and 1 mm in thickness as dielectric barrier with a discharge gap of 2 mm. A 0.15 g $Au/TiO_2$ catalyst (40–60 mesh) was loaded into the discharge gap region. Inlet gas centripetally flowed to the outlet that locates at the center of grounded electrode. High voltage with an AC frequency of 1.8 kHz and input power ($P_{in}$) of 3 W were applied. The voltage and current waveforms were monitored with an oscilloscope (DPO4108B, Tektronix) through a high-voltage probe (P6015A, Tektronix) and a sampling resistor (2.5 Ω), respectively. A wattmeter was installed in the primary side of the transformer to measure the input power. To in-situ regenerate the deactivated $Au/TiO_2$ catalyst by plasma, 200 mL/min synthetic air (20% $O_2$ balance $N_2$, used in Sections 3.1–3.4) or air (used in Section 3.5) with various water vapor contents flowed into the DBD reactor. Water vapor was carried by gas through a water bubbler in a water bath at room temperature. Water vapor content was measured online using a dew point hygrometer (653-2, Testo, Germany), and various water vapor contents were changed with the flow rates of carrier gas. Unless otherwise specified, the plasma regeneration time was set at 5 min. The gaseous products from plasma regeneration were online monitored using an FT-IR (IGS, Thermofisher, USA) equipped with a gas cell of 2 m in optical path length. Before the plasma regeneration, the FT-IR spectra of the synthetic air with a certain content of water vapor were collected to use as the background.

The activity of $Au/TiO_2$ catalyst was evaluated at room temperature in the DBD reactor with plasma off. A gas mixture of 1000 ppm CO, 20% $O_2$, 0.55% $H_2O$ balance $N_2$ was fed into the reactor at a GHSV of 80,000 mL $h^{-1}$ $g^{-1}$. Inlet and outlet gaseous products were online analyzed by a $CO_x$ analyzer (S710, Sick/Maihak, Germany). CO conversion ($X$) was calculated as shown below:

$$X = \frac{C_{CO}^{in} - C_{CO}^{out}}{C_{CO}^{in}} \quad (1)$$

where $C_{CO}^{in}$ and $C_{CO}^{out}$ represent the concentrations of CO in inlet and outlet gases, respectively.

### 2.2. Catalyst characterizations

The Au loading on $Au/TiO_2$ catalyst was about 0.8 wt.% determined by inductively coupled plasma-atomic emission spectroscopy (ICP-AES, Optima 2000DV, USA). The $Au/TiO_2$ sample of 50 mg was dissolved in aqua regia and then transferred into 25 mL volumetric flask for measurement. The standard solutions for ICP-AES measurement were purchased from GRINM.

The particle size of fresh, deactivated and regenerated catalysts was observed by transmission electron microscopy (TEM, Tecnai $G^2$ Spirit, Hong Kong) operating at 120 kV. The samples were prepared for TEM by first grounding them to fine powder, and then mixing about 40 mg of the fine powder with 5 mL ethanol to make a suspension for 30 min ultrasonic treatment. Five drops of the suspension were dripped on a copper mesh grid with holey carbon film, subsequently dried at room temperature for measurement. The distribution of particle size was calculated by counting more than 200 particles in different areas.

Diffuse reflectance UV–vis spectra were carried out on the air-exposed $Au/TiO_2$ powder samples using a JASCO UV-550 spectrometer in the wavelength range of 200–800 nm. A background reference was taken using barium sulfate before the measurement.

Surface chemical states of $Au/TiO_2$ catalysts were characterized by a X-ray photoelectron spectroscopy (XPS, ESCALAB250 Thermo VG, USA) using an Al Kα X-ray source (1486.6 eV) operated at 15 kV and 300 W with a pass energy of 50 eV.

## 3. Results

### 3.1. Plasma regeneration of $Au/TiO_2$ catalyst and effect of humidity

Under circumstances of humid or dry synthetic air (abbreviated as humid plasma or dry plasma below) as discharge gas for plasma regeneration of $Au/TiO_2$ catalysts, CO oxidation reaction was conducted firstly over the fresh $Au/TiO_2$ catalysts for 70 min to allow the catalysts deactivated at the same level. The deactivated catalysts were in-situ regenerated for 5 min by the humid plasma (in presence of 2.77% $H_2O$) and dry plasma at $P_{in}$ of 3 W and total flow rate ($F$) of 200 mL/min, respectively, over which CO oxidation reaction was conducted again to evaluate the performance of regenerated catalysts. Fig. 2 shows the CO conversion over the fresh and the regenerated $Au/TiO_2$ catalysts with TOS. As shown in Fig. 2, CO conversion over the fresh $Au/TiO_2$ catalyst gradually dropped from 91% to 69% with 70 min of TOS due to the accumu-

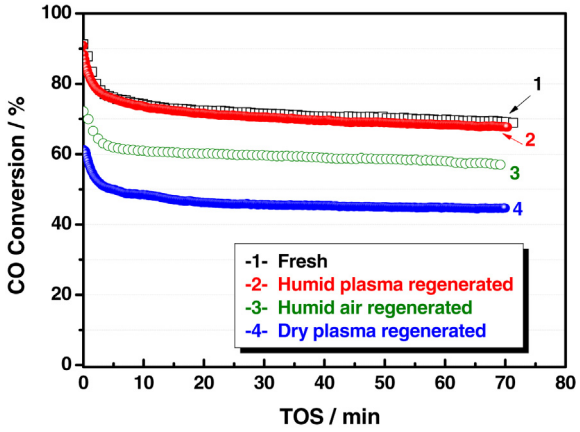


**Fig. 2.** CO conversion as a function of TOS over fresh $Au/TiO_2$ catalyst, and the regenerated $Au/TiO_2$ catalysts by humid plasma (in presence of 2.77% $H_2O$) and dry plasma. The sample regenerated by humid air without plasma was used for reference.

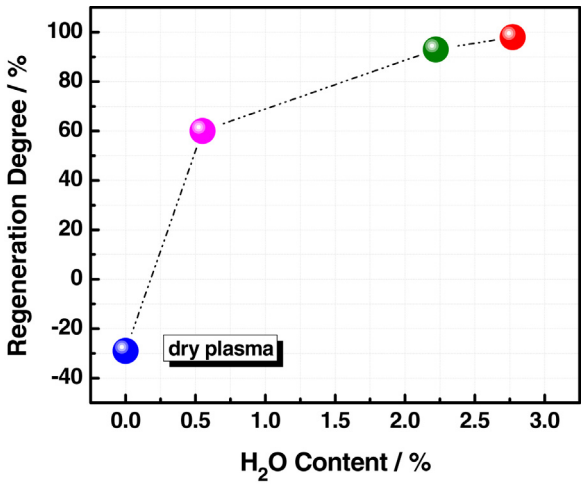


**Fig. 3.** Effect of water vapor content on regeneration degree of $Au/TiO_2$ catalysts.

lation of carbonate species on catalyst surface. Fig. 2 also shows that starting from the same level of deactivation, catalytic activity of $Au/TiO_2$ catalyst after the humid plasma regeneration for a fixed regeneration time was distinctive from that of dry plasma. After the humid plasma regeneration, the catalyst was recovered completely, while after the dry plasma regeneration, the catalyst unexpectedly became worse than and its catalytic activity was remarkably inferior to that before regeneration. Furthermore, considering that water vapor can favor the decomposition of surface carbonate species on Au catalyst [31–33], thus the regeneration by humid synthetic air (2.77% $H_2O$ and $F$ = 200 mL/min) without plasma was conducted for the same time as a reference experiment. From Fig. 2, it can be clearly seen that the CO conversion of the catalyst regenerated by the humid air was slightly increased from 69% (before regeneration) to 72% (after regeneration). This means that, if without plasma, water vapor has only a very weak effect on the catalyst regeneration.

To quantify the regeneration ratio of the deactivated catalysts, a parameter of regeneration degree is defined as below.

$$\text{regeneration degree} = \frac{X_{\text{reg}}^{\max} - X_{\text{fresh}}^{\min}}{X_{\text{fresh}}^{\max} - X_{\text{fresh}}^{\min}} \quad (2)$$

where $X_{\text{fresh}}^{\max}$ and $X_{\text{reg}}^{\max}$ represents the maximum CO conversion of the fresh and the regenerated catalysts, respectively. They also refer to the initial activity [36]. $X_{\text{fresh}}^{\min}$ denotes the minimum CO conversion of the fresh catalyst before plasma regeneration, which stands for the activity of the fresh catalyst after 70 min reaction as shown in Fig. 2.

As shown in Fig. 3, regeneration degree is strongly dependent on water vapor content in air plasma. Starting from the same deactivation level of the catalyst followed by a fixed time of regeneration, the regeneration degree increased rapidly from negative 29% to positive 60% when the discharge gas was switched from dry gas to humid gas in presence of 0.55% $H_2O$, and reached 98% at water vapor content of 2.77% indicating the catalyst being almost completely regenerated. If without plasma, the regeneration degree of the humid air (2.77% $H_2O$) was only 14%. It is worth noting that the negative regeneration degree of dry plasma was attributed to the catalyst poisoning derived from nitrogen oxides during dry plasma regeneration [24]. Apparently, there should be a significant contribution of water vapor to improved regeneration performance of the deactivated $Au/TiO_2$ catalyst. To better understand the mechanism of improved regeneration degree due to contribution of water vapor, electric discharge characteristics, gaseous product during the humid and dry plasma regeneration, and regenerated catalyst characterizations certainly were of interest to investigate.

### 3.2. Electric discharge characteristics

To gain an insight into the plasma regeneration process, the discharge voltage and current, and Lissajous figure in humid and dry plasmas are shown in Fig. 4. Compared with the dry plasma at the same input power, voltage amplitude in humid plasma decreased, but the corresponding current amplitude increased. Moreover, numerous and intense current pulses of microdischarge per half voltage cycle in dry plasma can be clearly observed from Fig. 4a, which indicates a typical filamentary DBD mode in the dry plasma [37,38]. In contrast, for the humid plasma in presence of 2.77% $H_2O$, the current pulse weakened greatly and a broad peak of discharge current per half voltage cycle appeared as shown in Fig. 4b, which is similar to current waveform of atmospheric pressure glow discharge in open air [39]. Generally, the generation of a glow discharge in air at atmospheric pressure mainly depends on the configuration of dielectric barrier, electrode geometry and gas flow rate [39–41]. Garamoon and El-zeer [39] reported atmospheric pressure glow discharge in air using porous alumina as dielectric barrier, and Wang et al. [40] achieved a homogeneous looking discharge in air at atmospheric pressure using mesh electrode. However, in this study, the relatively uniform DBD mode of humid plasma is mainly ascribed to the contribution of water vapor because the current pulses of microdischarge gradually become less and weaker with increasing water vapor content. Furthermore, Falkenstein et al. [42] and Messaoudi et al. [43] reported that the presence of water vapor in air can reduce the surface resistance of dielectric and increase the effective dielectric capacity, which would not only result in the discharge transformation from filamentary mode to the relatively uniform mode, but also lead to the change of Lissajous figure shape and its enclosed area. Also, the enclosed area is proportional to the discharge power. As a result, with the change from dry plasma to humid plasma for regeneration as shown in Fig. 4c, the shape of Lissajous figure transformed from parallelogram to ellipse, and the corresponding discharge power increased from 0.7 W to 1.4 W at $P_{\text{in}}$ of 3 W. This means that the presence of water vapor leads to the increase in the efficiency of electrical energy transfer to the plasma. It should be noted that, if the discharge power increases by raising the input power in dry plasma regeneration, the regeneration performance will become worse because of the occurrence of much intenser microdischarges.

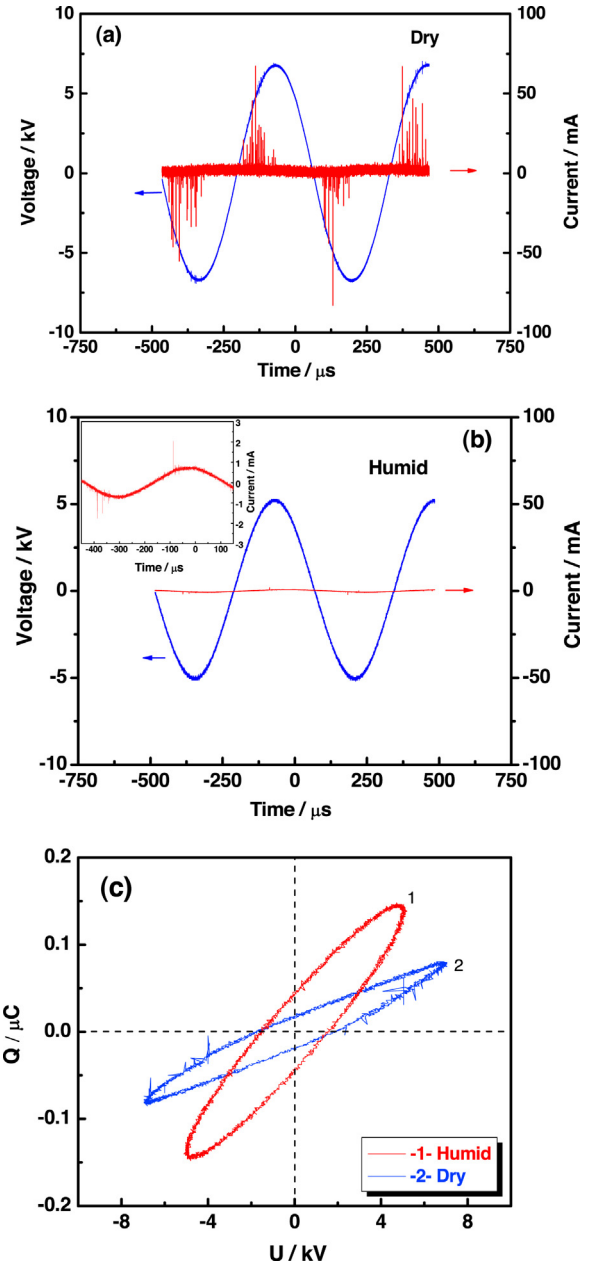


**Fig. 4.** Waveforms of discharge voltage and current of dry plasma (a) and humid plasma (b) regeneration and their Lissajous figure (c). Inset of (b): enlarged current waveform.

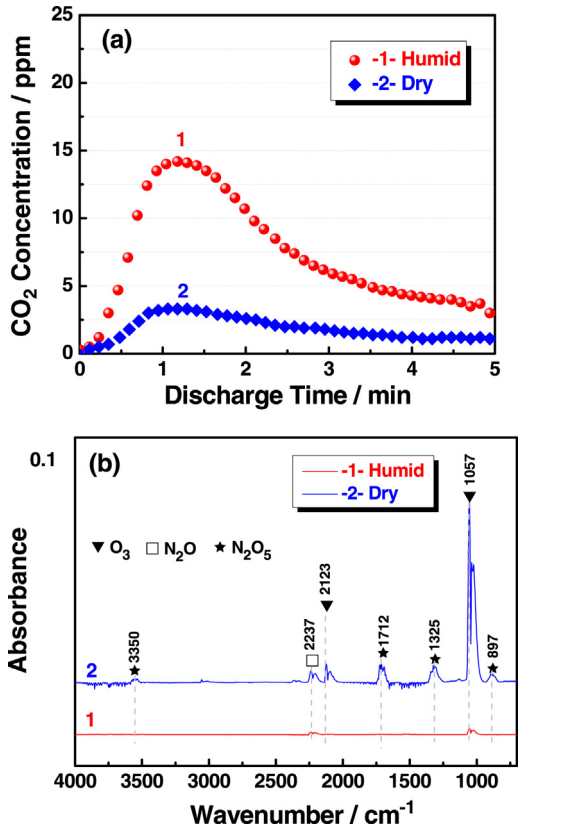


**Fig. 5.** Concentration of $CO_2$ released versus discharge time (a) and FT-IR spectra (b) during humid plasma (in presence of 2.77% $H_2O$) and dry plasma regeneration. The sample used for the regeneration was taken from the deactivated catalyst after 70 min CO oxidation reaction.

### 3.3. Analysis of gaseous products during plasma regeneration

Fig. 5a shows variation in the concentration of $CO_2$ released from the deactivated catalyst with discharge time during humid plasma (in presence of 2.77% $H_2O$) and dry plasma regeneration ($P_{in}$ = 3 W and $F$ = 200 mL/min). The $Au/TiO_2$ catalysts at the same level of deactivation were obtained from the fresh catalysts after 70 min CO oxidation, which was designed in purpose of ensuring that the same amount of carbonate species were accumulated on Au catalyst surface. As shown in Fig. 5a, the concentration of $CO_2$ released from the humid plasma regeneration dramatically increased in comparison with the dry plasma regeneration, which means much more $CO_2$ was released from humid plasma regeneration. This evidence manifests that the presence of water vapor in humid plasma regeneration facilitates the decomposition of carbonate species on catalysts surface. Combined with the results as shown in Fig. 2, it can be deduced that nearly all the deactivated active sites of the catalyst were regenerated in humid plasma within 5 min of regeneration time.

Additionally, based upon our previous work [24], Au nanocatalysts can be poisoned by the byproduct of nitrogen oxides except $N_2O$ produced from the plasma regeneration. Therefore, nitrogen oxides produced from humid plasma and dry plasma regeneration were online analyzed by FT-IR. As shown in Fig. 5b, only $N_2O$ with the characteristic IR band at 2237 $cm^{-1}$ was detected from humid plasma regeneration. However, besides $N_2O$, $N_2O_5$ with the IR bands at 897 $cm^{-1}$, 1325 $cm^{-1}$, 1712 $cm^{-1}$ and 3350 $cm^{-1}$, which is the severest poisoning species of nitrogen oxides [24], was remarkably detected from dry plasma regeneration. Therefore, the poor regeneration performance of dry plasma regeneration was attributed to relatively low decomposition rate of carbonate species and the formation of $N_2O_5$, while $N_2O_5$ was not detected and the intensity of $O_3$ (1057 $cm^{-1}$) and $N_2O$ also dramatically decreased for humid plasma regeneration, as shown in Fig. 5b.

### 3.4. Characterizations of Au catalysts

Because of the distinct surface plasmon resonance of gold nanoparticle, UV–vis spectroscopy is well suited to characterize $Au/TiO_2$ catalysts. Fig. 6 shows the diffuse reflectance UV–vis spectra of the fresh, the deactivated and the regenerated by humid plasma and dry plasma $Au/TiO_2$ catalysts. Obviously, the typical plasmon band of metallic Au particle between 500 nm and 600 nm can be clearly observed for the fresh and the regenerated samples by humid plasma from Fig. 6 [44–46], and the bandwidth of the regenerated sample by humid plasma is very close to that of the fresh catalyst. This suggests that the humid plasma can effectively

**Table 1**
XPS analysis of $Au/TiO_2$ samples.

| Samples | B.E. Au $4f_{7/2}$ (eV) | | $Au^{\delta+}/(Au^{\delta+}+Au^0)$ (at.%) | $[OH]_s/([H_2O]_a+[OH]_s+[O]_l)$ (at.%) |
|---|---|---|---|---|
| | $Au^0$ | $Au^{\delta+}$ | | |
| a | 83.3 | 85.4 | 20 | 11 |
| b | 83.3 | 85.4 | 16 | 16 |
| c | 83.3 | 85.5 | 15 | 20 |
| d | 83.7 | 85.9 | 15 | 10 |

*Note:* samples a, b, c and d represent the fresh and the deactivated catalyst, and the regenerated catalysts by humid plasma and dry plasma, respectively.

remove the accumulated carbonate species and inhibits simultaneously the formation of nitrogen oxides, which is consistent with the results in Section 3.3. However, for the deactivated sample, its bandwidth showed a remarkable broadening in comparison with the fresh catalyst. This is due to that the surrounding chemical environment of gold particle was changed by the carbonate species accumulated on catalyst surface. Moreover, the regenerated sample by dry plasma presented the widest bandwidth because of the formation of surface poisoning species $[NO_y]_s$ on $Au/TiO_2$ catalyst derived from nitrogen oxides [24]. Generally, the change of bandwidth is not only related to the particle size distribution but also correlates with the dielectric function of supporting or surrounding [47–49]. Here the broadening bandwidth arises from the change in chemical environment but not Au particle size, which is evidenced by TEM results as shown in Fig. 7. Compared to the fresh sample, the Au particle sizes of the deactivated and the regenerated samples by humid and dry plasma showed no distinct change and all averaged at around 3.5 nm. This confirmed that there was no obvious aggregation during the deactivated process and the regeneration processes by dry plasma and humid plasma.

To determinate the changes in chemical environment of $Au/TiO_2$ catalyst surface derived from the deactivation and plasma regeneration, the high resolution XPS spectra of N 1s, O 1s, Ti 2p and Au 4f of the fresh, the deactivated and the regenerated by dry plasma and humid plasma $Au/TiO_2$ catalysts are shown in Fig. 8. In N 1s spectra, the peaks at 399.4 eV assigned to the molecularly chemisorbed $\gamma$-$N_2$[37] were all observed for the four samples. However, only the regenerated sample by dry plasma appeared a new peak at 406.6 eV, which derives from the formation of $[NO_y]_s$ on catalyst surface [24,50]. This indicates that the humid plasma could avoid the formation of poisoning species $[NO_y]_s$ in comparison with the dry plasma, which is in good line with the FT-IR and UV–vis spectra results. In O 1s spectra, the distribution of the oxygen species on $Au/TiO_2$ catalysts surface were calculated and summarized in Table 1 base on the deconvolution results. Both lattice oxygen $[O]_l$ and hydroxyl groups $[OH]_s$ appeared in all samples.

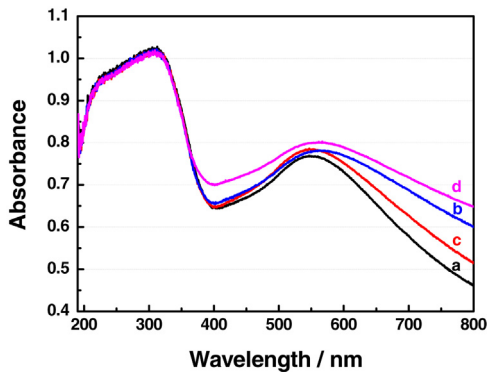


**Fig. 6.** Diffuse reflectance UV–vis spectra of the fresh (a), the deactivated (b), and the regenerated by the humid plasma (c) and dry plasma (d) $Au/TiO_2$ catalysts.

The regenerated sample by humid plasma showed adsorbed water $[H_2O]_a$ peak at 533.2 eV [51,52] and showed the highest content of $[OH]_s$ (Table 1) due to the presence of water vapor in humid plasma regeneration. The Au 4f spectra can be deconvoluted into $Au^0$ and $Au^{\delta+}$ components [53,54], and the corresponding results are also listed in Table 1. The $Au^0$ content shows a little increase in the deactivated and the regenerated catalysts, which is likely caused by the gradual reduction of $Au^{\delta+}$ during CO oxidation. Compared with other samples, Au 4f peaks of the regenerated sample by dry plasma shifted to higher binding energy by 0.4 eV. Similar +0.3 eV shift of Ti 2p peaks for this sample was also observed from Fig. 8. Apparently, the formation of strong electron-withdrawing species $[NO_y]_s$ on catalyst surface [55] during dry plasma regeneration inevitably leads to a blue shift of Au and Ti binding energy.

### 3.5. *In-situ plasma regeneration using normal air instead of synthetic air*

In the above-mentioned experiments, synthetic air was employed for plasma regeneration. To ensure if it is practical for the plasma regeneration, in-situ regeneration using normal air instead of synthetic air was conducted in the following experiments.

The CO conversion versus TOS over the fresh and the regenerated $Au/TiO_2$ catalysts by humid air (in presence of 2.77% $H_2O$) plasma is shown in Fig. 9. The activity of the fresh $Au/TiO_2$ catalyst reduced gradually with TOS. After 12 h of TOS, the CO conversion reduced from initial 92% to 40%. As expected, the deactivated catalyst after the long-term reaction was in-situ regenerated by humid air plasma for 10 min, the catalyst activity was almost fully recovered.

Fig. 10 shows the regeneration degree of $Au/TiO_2$ catalyst by humid air plasma in 10 deactivation-regeneration cycles. The experiment of a single cycle was conducted as following. CO oxidation reaction over the $Au/TiO_2$ catalyst run for 70 min, and the catalyst was in-situ regenerated by humid air plasma for 5 min. The regeneration degree in ten deactivation-regeneration cycles ranged between 94% and 100%, and verified that the regenerated $Au/TiO_2$ catalyst was durable by humid air plasma.

In view of the excellent regeneration performance by humid air plasma, it is reasonable to believe that in-situ regeneration of Au nanocatalysts by atmospheric-pressure air plasma is a fast, facile and economical technology for practical applications.

## 4. Discussion

### 4.1. *Deactivation of Au catalyst*

Results shown in Fig. 2 clearly demonstrated that the deactivation phenomenon of $Au/TiO_2$ catalysts existed during CO oxidation, which has also been reported in literatures [13–17]. It is generally accepted that the Au particle growth and the accumulation of carbonate species on Au catalyst surface are two major reasons for the deactivation phenomenon [16,17]. The Au particle sizes change induced by the reaction heat during CO oxidation at room temperature is negligible [13,14,30], which is supported by the similar Au particle sizes between fresh and deactivated $Au/TiO_2$ catalysts (Fig. 7). Therefore, the activity loss of the Au catalyst is attributed to the accumulation of surface carbonate species in this study. The mechanism for the buildup of carbonate species on catalyst surface can be described briefly as the following. Low-temperature CO catalytic oxidation on $Au/TiO_2$ catalysts follows the Langmuir–Hinshelwood mechanism, with both CO and $O_2$ adsorbed on the catalyst surface [12,56]. CO adsorbs on the Au particles, while molecular oxygen probably adsorbs on oxygen vacancies of $TiO_2$ as a superoxide ($O_2^-$) species, which would readily

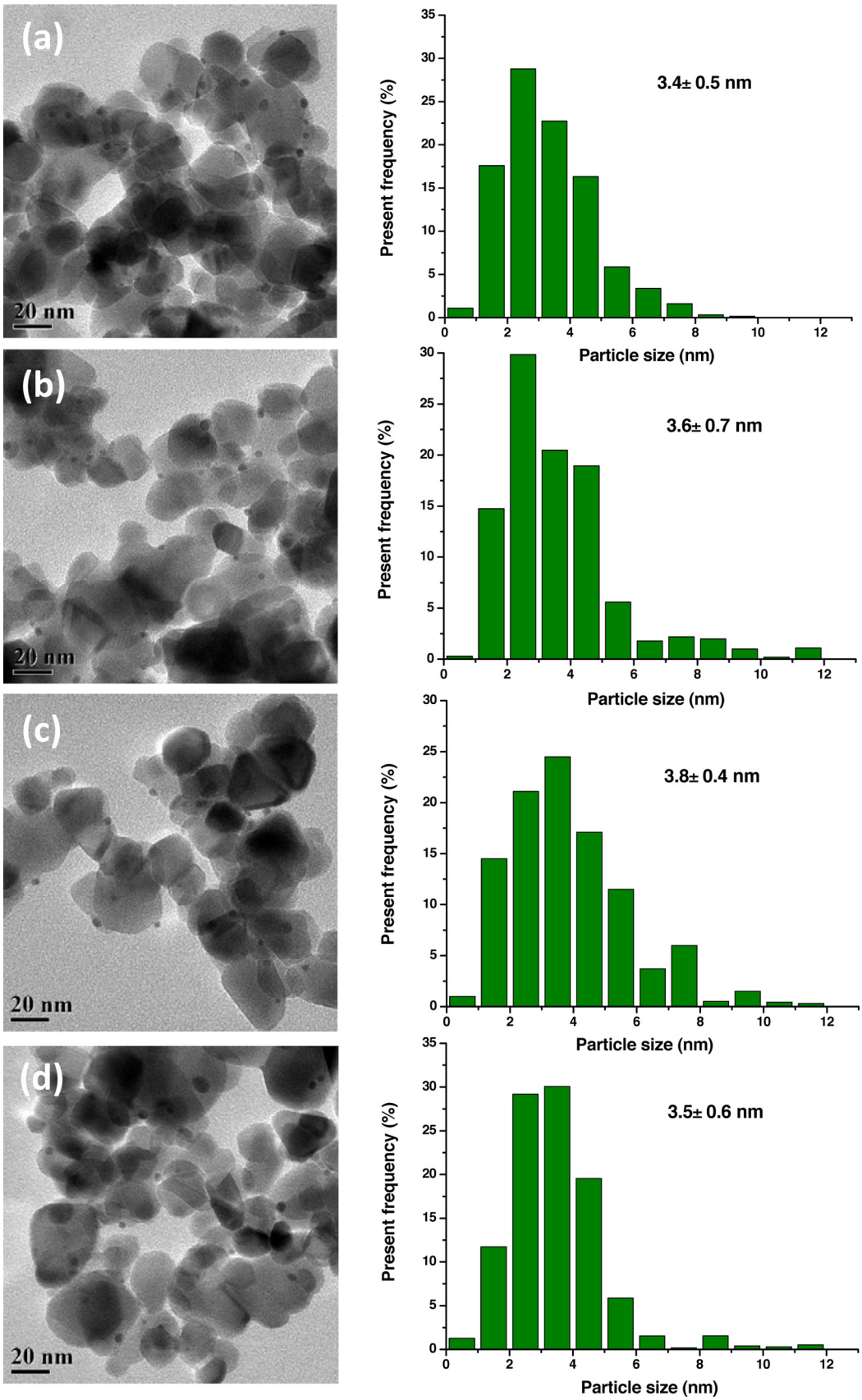


**Fig. 7.** TEM images of the fresh (a), the deactivated (b) and the regenerated by humid plasma (c) and dry plasma (d) $Au/TiO_2$ catalysts.

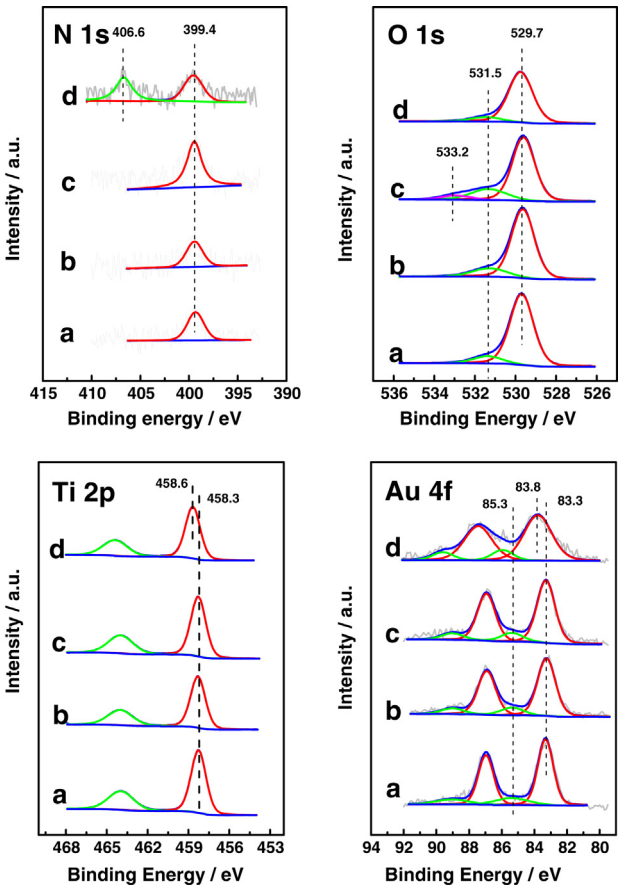


**Fig. 8.** XPS spectra of the fresh (a), the deactivated (b) and the regenerated by the humid plasma (c) and dry plasma (d) $Au/TiO_2$ catalysts.

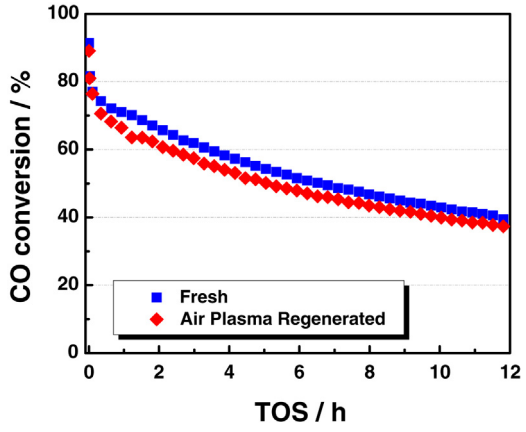


**Fig. 9.** CO conversion as a function of TOS over the fresh $Au/TiO_2$ catalyst and the regenerated catalyst by air plasma.

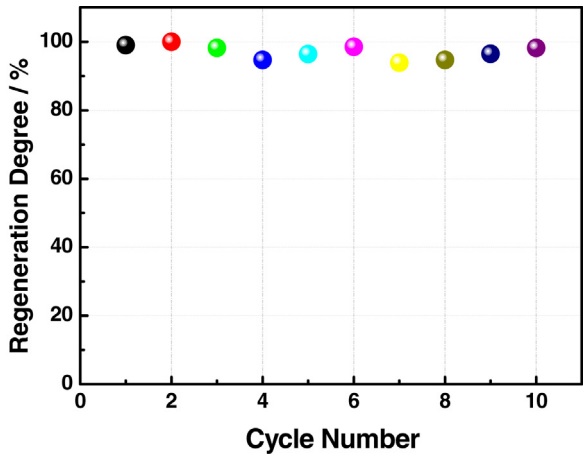


**Fig. 10.** Regeneration degree of $Au/TiO_2$ catalyst by humid air plasma in 10 deactivation-regeneration cycles.

mobile to the metal-support interface due to its high surface mobility [57,58]. The superoxide ($O_2^-$) species on the interface can directly or indirectly (via dissociation to active oxygen atom) react with the absorbed CO to form intermediate on the interface [56,57,59]. Moreover, Saavedra et al. [60] recently present a mechanism that the Au-OOH species derived from activated $O_2$ on metal-support interface can readily react with the adsorbed Au-CO on Au particles to form Au-COOH. Anyway, if the formed intermediate on Au catalyst surface immediately decomposes into $CO_2$, the active site can be liberated and the CO oxidation proceeds. But if the intermediate converts into inert carbonate species, which deposits on the interface and even migrates to $TiO_2$ support, the activity of the Au catalyst would gradually decrease because the active sites are occupied [14–16].

### 4.2. Regeneration of Au catalyst by air plasma

On the basis of the above deactivation discussion, it can be deduced that the deactivated Au catalyst could be regenerated if the accumulated carbonate species were effectively removed. As a promising technique, plasma has been successfully employed to regenerate deactivated Au catalyst by using pure oxygen as discharge gas [17,24]. From the practical point of view, the goal of this work is to regenerate the deactivated Au catalyst by air plasma. In fact, according to our previous work [24], the dry air plasma cannot be used to regenerate the Au catalyst due to the serious poisoning effect caused by nitrogen oxides. For the poisoning effect during air plasma regeneration, it was mainly attributed to that poisoning species $[NO_y]_s$ derived from that nitrogen oxides (except $N_2O$) occupy the oxygen vacancies of $TiO_2$ and block the adsorption of oxygen molecules [24].

With respect to the reaction kinetics of nitrogen oxides formation in non-thermal plasma, it is well known that the formation of NO follows Zeldovich mechanism [61].

$$O + N_2(X, v) \rightarrow NO + N \quad (R1)$$

$$N + O_2 \rightarrow NO + O \quad (R2)$$

The reaction (R1) of highly vibrationally excited $N_2(X, v)$ with O atom can efficiently proceed to break the N—N bond of $N_2$ molecule because of its very high bonding energy (9.8 eV/molecule). The energy is required to overcome the high activation energy (~3 eV/molecule) of reaction (R1). After $N_2$ dissociation, NO is formed in the exothermic reaction (R2). In the mechanism of chain propagation, reaction (R2) is limited by the strongly endothermic formation of N atoms in reaction (R1) [61]. The required energy of reaction (R1) can be provided by the intense current pulse of filamentary mode in dry plasma regeneration. Once NO is produced, it can be further oxidized easily in plasma and finally to form $N_2O_5$. In humid plasma regeneration, the discharge approaches a uniform mode with a little and very weak current pulses and the formation of NO is prevented accordingly. Therefore, $N_2O_5$ was produced in dry plasma while not the case in humid plasma, which is evidenced by the results of FT-IR (Fig. 5b), diffuse reflectance UV–vis (Fig. 6) and XPS (Fig. 8) spectra. Consequently, in humid plasma regeneration, there is no the poisoning effect of nitrogen oxides. In dry

plasma regeneration, a small amount of the carbonate species was decomposed to $CO_2$ released from catalyst surface (Fig. 5a), but the nitrogen oxides species on Au catalyst had much more poisoning effect on regeneration process. Therefore, the dry plasma gave a very negative regeneration degree (Fig. 3).

As for the decomposition of carbonate species on catalyst surface, the humid plasma significantly accelerated this process as compared to the dry plasma (Fig. 5b), and the contribution of water vapor on speeding up carbonate species decomposition in plasma regeneration can be interpreted as the following.

The presence of water vapor in air (humid air) can directly decompose the surface carbonate species to a small extent [18,29,33,62]. As shown in Fig. 2, the catalytic activity can be slightly recovered by humid air (without plasma). Generally, water vapor decomposing the carbonate species follows a hydrolysis model [33,62], which is shown in Eqs. (R3) and (R4).

$$[CO_3]_s + [H_2O]_s \rightarrow [CO_3H]_s + [OH]_s \quad \text{(R3)}$$

$$[CO_3H]_s \rightarrow CO_2(g) + [OH]_s \quad \text{(R4)}$$

Inert carbonate species ($[CO_3]_s$) on the metal (Au)-support ($TiO_2$) interface were nucleophilic attacked by surface absorbed water ($[H_2O]_s$) to form bicarbonate species ($[CO_3H]_s$), and then the formed bicarbonate species further decomposed to evolve gaseous product $CO_2$ and the occupied sites were liberated. However, if without plasma, water vapor has only a very weak effect on the catalyst regeneration, as illustrated in Fig. 2.

In humid plasma regeneration, the presence of water vapor leads to the relatively uniform DBD mode (Fig. 4b) and the increase of discharge power (Fig. 4c), which greatly facilitates the decomposition of carbonate species on catalyst surface. The relatively uniform discharge and the increase in discharge power results in that the energy can be more effectively and uniformly coupled into the humid plasma at the same input power, which is advantageous to producing a large amount of active species for regeneration. Meanwhile, the relatively uniform discharge would make the active species evenly spread out over the deactivated catalyst, which is beneficial to removing all of the accumulated carbonate species from catalyst surface.

## 5. Conclusions

In-situ regeneration of the deactivated $Au/TiO_2$ nanocatalysts during CO oxidation reaction by atmospheric-pressure cold plasma of air was explored. A significant contribution of water vapor in enhanced regeneration performance of Au catalysts by air plasma was surprisingly observed. After plasma regeneration of the catalysts for 5 min, the regeneration degree significantly increased up to 98% under humid plasma in presence of 2.77 vol.% $H_2O$, but decreased down to negative 29% under dry plasma.

As evidenced by the analyses of electric discharge characteristics and gaseous products and the catalyst charaterizations of diffuse reflectance UV–vis and XPS spectra, water vapor facilitates the decomposition of carbonate species on the deactivated catalysts and simultaneously inhibits the formation of poisoning species of nitrogen oxides during air plasma regeneration. The benefits of water vapor in air plasma regeneration mainly originate from the increase in the efficiency of electrical energy transfer to the plasma and the characteristic of the relatively uniform discharge.

Furthermore, normal air instead of synthetic air in humid plasma regeneration was implemented on the evaluations of the deactivated Au catalysts after a long-term reaction and during ten deactivation-regeneration cycles, which successfully demonstrated in-situ regeneration of Au nanocatalysts by atmospheric-pressure air plasma as a fast, facile and economical technology.

## Acknowledgments

This work is supported by National Natural Science Foundation of China (11175036, U1201231) and the Fundamental Research Funds for the Central Universities (DUT14RC(3)012).

## References

[1] M. Haruta, Gold bull. 37 (2004) 27–36.
[2] J. Gong, Chem. Rev. 112 (2011) 2987–3054.
[3] K. Christmann, S. Schwede, S. Schubert, W. Kudernatsch, ChemPhysChem 11 (2010) 1344–1363.
[4] M. Kipnis, Appl. Catal. B 152–153 (2014) 38–45.
[5] S. Scirè, L.F. Liotta, Appl. Catal. B 125 (2012) 222–246.
[6] S.A. Nikolaev, E.V. Golubina, I.N. Krotova, M.I. Shilina, A.V. Chistyakov, V.V. Kriventsov, Appl. Catal. B 168–169 (2015) 303–312.
[7] P. Sudarsanam, B. Mallesham, P.S. Reddy, D. Großmann, W. Grünert, B.M. Reddy, Appl. Catal. B 144 (2014) 900–908.
[8] A. Sandoval, C. Louis, R. Zanella, Appl. Catal. B 140–141 (2013) 363–377.
[9] S. Royer, D. Duprez, ChemCatChem 3 (2011) 24–65.
[10] W. Li, M. Comotti, F. Schüth, J. Catal. 237 (2006) 190–196.
[11] Y. Denkwitz, M. Makosch, J. Geserick, U. Hörmann, S. Selve, U. Kaiser, N. Hüsing, R.J. Behm, Appl. Catal. B 91 (2009) 470–480.
[12] B.K. Min, C.M. Friend, Chem. Rev. 107 (2007) 2709–2724.
[13] A. Karpenko, R. Leppelt, J. Cai, V. Plzak, A. Chuvilin, U. Kaiser, R.J. Behm, J. Catal. 250 (2007) 139–150.
[14] Y. Denkwitz, B. Schumacher, G. Kučerová, R.J. Behm, J. Catal. 267 (2009) 78–88.
[15] P. Konova, A. Naydenov, T. Tabakova, D. Mehandjiev, Catal. Commu. 5 (2004) 537–542.
[16] P. Konova, A. Naydenov, C. Venkov, D. Mehandjiev, D. Andreeva, T. Tabakova, J. Mol. Catal. A: Chem. 213 (2004) 235–240.
[17] H.H. Kim, S. Tsubota, M. Daté, A. Ogata, S. Futamura, Appl. Catal. A 329 (2007) 93–98.
[18] H.S. Oh, C.K. Costello, C. Cheung, H.H. Kung, M.C. Kung, Stud. Surf. Sci. Catal. 139 (2001) 375–381.
[19] J. Van Durme, J. Dewulf, C. Leys, H. Van Langenhove, Appl. Catal. B 78 (2008) 324–333.
[20] H.-H. Kim, Y. Teramoto, T. Sano, N. Negishi, A. Ogata, Appl. Catal. B 166–167 (2014) 9–17.
[21] H.L. Chen, H.M. Lee, S.H. Chen, M.B. Chang, S.J. Yu, S.N. Li, Environ. Sci. Technol. 43 (2009) 2216–2227.
[22] X. Liu, C.Y. Mou, S. Lee, Y. Li, J. Secrest, B.W.L. Jang, J. Catal. 285 (2012) 152–159.
[23] Z.H. Wei, C.J. Liu, Mater. Lett. 65 (2011) 353–355.
[24] H.Y. Fan, C. Shi, X.S. Li, S. Zhang, J.L. Liu, A.M. Zhu, Appl. Catal. B 119–120 (2012) 49–55.
[25] R. Peyrous, P. Pignolet, B. Held, J. Phys. D: Appl. Phys. 22 (1989) 1658–1667.
[26] D. Braun, U. Küchler, G. Pietsch, Pure Appl. Chem. 60 (1988) 741–746.
[27] R. Peyrous, Ozone Sci. Eng. 12 (1990) 41–64.
[28] B. Schumacher, Y. Denkwitz, V. Plzak, M. Kinne, R.J. Behm, J. Catal. 224 (2004) 449–462.
[29] M. Daté, M. Haruta, J. Catal. 201 (2001) 221–224.
[30] J. Saavedra, C. Powell, B. Panthi, C.J. Pursell, B.D. Chandler, J. Catal. 307 (2013) 37–47.
[31] M.M. Schubert, A. Venugopal, M.J. Kahlich, V. Plzak, R.J. Behm, J. Catal. 222 (2004) 32–40.
[32] J.T. Calla, R.J. Davis, J. Catal. 241 (2006) 407–416.
[33] M. Daté, M. Okumora, S. Tsubota, M. Haruta, Angew. Chem. Int. Ed. 43 (2004) 2129–2132.
[34] M. Ojeda, B.-Z. Zhan, E. Iglesia, J. Catal. 285 (2012) 92–102.
[35] L. Delannoy, N.E. Hassan, A. Musi, N.N. Le To, J.-M. Krafft, C. Louis, J. Phys. Chem. B 110 (2006) 22471–22478.
[36] S. Zhang, X.-S. Li, B. Chen, X. Zhu, C. Shi, A.-M. Zhu, ACS Catal. 4 (2014) 3481–3489.
[37] U. Kogelschatz, IEEE Trans. Plasma Sci. 30 (2002) 1400–1408.
[38] J. Ráhel, D.M. Sherman, J. Phys. D: Appl. Phys. 38 (2005) 547–554.
[39] A.A. Garamoon, D.M. El-zeer, Plasma Sources Sci. Technol. 18 (2009) 045006.
[40] X. Wang, H. Luo, Z. Liang, T. Mao, R. Ma, Plasma Sources Sci. Technol. 15 (2006) 845–848.
[41] P. Rajasekaran, P. Mertmann, N. Bibinov, D. Wandke, W. Viöl, P. Awakowicz, Plasma Process Polym 7 (2010) 665–675.
[42] Z. Falkenstein, J.J. Coogan, J. Phys. D: Appl. Phys. 30 (1997) 817–825.
[43] R. Messaoudi, A. Younsi, F. Massines, B. Despax, C. Mayoux, IEEE Trans. Dielectr. Electr. Insul. 3 (1996) 537–543.
[44] R. Zanella, S. Giorgio, C.H. Shin, C.R. Henry, C. Louis, J. Catal. 222 (2004) 357–367.
[45] A.C. Gluhoi, N. Bogdanchikova, B.E. Nieuwenhuys, J. Catal. 232 (2005) 96–101.
[46] J. Huang, W.L. Dai, H. Li, K. Fan, J. Catal. 252 (2007) 69–76.
[47] P. Claus, A. Brückner, C. Mohr, H. Hofmeister, J. Am. Chem. Soc. 122 (2000) 11430–11439.
[48] K.-J. Berg, A. Berger, H. Hofmeister, Z. Phys D: At. Mol. Clusters 20 (1991) 309–311.
[49] D. Schönauer, H. Lauer, U. Kreibig, Z. Phys D: At. Mol. Clusters 20 (1991) 301–304.

[50] C. Chen, H. Bai, C. Chang, J. Phys. Chem. C 111 (2007) 15228–15235.
[51] J. Pouilleau, D. Devilliers, F. Garrido, S. Durand-Vidal, E. Mahé, Mater. Sci. Eng. B 47 (1997) 235–243.
[52] J. Mizera, N. Spiridis, R. Socha, R. Grabowski, K. Samson, J. Korecki, B. Grzybowska, J. Gurgul, L. Kępiński, M.A. Małecka, Catal. Today 187 (2012) 20–29.
[53] L. Liu, X. Gu, Y. Cao, X. Yao, L. Zhang, C. Tang, F. Gao, L. Dong, ACS Catal. 3 (2013) 2768–2775.
[54] Q. Fu, H. Saltsburg, M. Flytzani-Stephanopoulos, Science 301 (2003) 935–938.
[55] B.P. Dailey, J.N. Shoolery, J. Am. Chem. Soc. 77 (1955) 3977–3981.
[56] D. Widmann, R. Behm, Acc. Chem. Res. 47 (2014) 740–749.
[57] H. Liu, A.I. Kozlov, A.P. Kozlova, T. Shido, K. Asakura, Y. Iwasawa, J. Catal. 185 (1999) 252–264.
[58] M.M. Schubert, S. Hackenberg, A.C. van Veen, M. Muhler, V. Plzak, R.J. Behm, J. Catal. 197 (2001) 113–122.
[59] S. Carrettin, Y. Hao, V. Aguilar-Guerrero, B.C. Gates, S. Trasobares, J.J. Calvino, A. Corma, Chem.Eur. J. 13 (2007) 7771–7779.
[60] J. Saavedra, H.A. Doan, C.J. Pursell, L.C. Grabow, B.D. Chandler, Science 345 (2014) 1599–1602.
[61] A. Fridman, Plasma Chemistry, first ed., Cambridge University Press, New York, 2008.
[62] C.K. Costello, J.H. Yang, H.Y. Law, Y. Wang, J.N. Lin, L.D. Marks, M.C. Kung, H.H. Kung, Appl. Catal. A 243 (2003) 15–24.